Hindawi
International Journal of Energy Research
Volume 2024, Article ID 2941404, 15 pages
https://doi.org/10.1155/2024/2941404

Research Article

Optimal Sizing and Management of Hybrid Wind Turbine-Diesel-Battery System for Reverse Osmosis Seawater Desalination in NEOM City

Mohamed K. Hassan,[1] **Hegazy Rezk**,[2] **Hamdy Youssef**,[1] **Ahmed S. Shehata**,[3] **Alaa A. El-Bary**,[4] **and Ayman Al-Quraan**[5]

[1]*Mechanical Engineering Department, College of Engineering and Islamic Architecture, Umm Al-Qura University, Makkah 21955, Saudi Arabia*
[2]*Department of Electrical Engineering, College of Engineering in Wadi Alddawasir, Prince Sattam bin Abdulaziz University, Wadi Alddawasir, Saudi Arabia*
[3]*Marine Engineering Department, College of Engineering and Technology, Arab Academy for Science Technology and Maritime Transport, P.O. Box 1029, Alexandria, Egypt*
[4]*Basic and Applied Science Institute, Arab Academy for Science, Technology and Maritime Transport, P.O. Box 1029, Alexandria, Egypt*
[5]*Electrical Power Engineering Department, Hijjawi Faculty for Engineering Technology, Yarmouk University, Irbid 21163, Jordan*

Correspondence should be addressed to Ayman Al-Quraan; aymanqran@yu.edu.jo

Received 5 January 2024; Revised 6 March 2024; Accepted 26 April 2024; Published 16 May 2024

Academic Editor: Yashwant Sawle

Optimal sizing and management of hybrid wind turbine-diesel-battery system for reverse osmosis seawater desalination in NEOM city is the objective of the paper. Therefore, the paper explored the different factors to optimize and introduce a technoeconomic evaluation and energy management of a stand-alone wind turbine (WT) system, diesel generator (DG), and battery storage (BS). The suggested WT/DG/BS system is implemented to feed seawater reverse osmosis (SWRO) unit in NEOM. The necessitated desalinated water per day is 100 m^3. To determine the optimal size of WT/DG/BS corresponding to the minimum cost of energy (COE) and net present cost, two different ratings of the SWRO units (SWRO-100 and SWRO-150), three control dispatch strategies (load following, cycle charging, and combined dispatch), and five types of batteries are considered. HOMER software is performed to simulate and optimize the WT/DG/BS. The optimization results indicated that the best battery storage is the Trojan SAGM battery. In this case, the COE ranged between $0.337/kWh and $0.564/kWh. The lowest COE of $0.377/kWh is obtained when using a combined control strategy and SWRO-100 unit, whereas the worst COE of $0.564/kWh is obtained when using load following control strategy and SWRO-150 unit. The best option of the WT/DG/BS system to supply the SWRO unit is option number 26. This system includes one wind turbine of 90 kW, DG of 25 kW, 47 Trojan SAGM batteries, a 23.8 kW converter, a SWRO-100 unit, and a combined control strategy. The net present cost and the initial cost are $950,725 and $221,495, respectively. The annual operating cost and annual consumed fuel are $56,409 and 36,396 L, respectively. Compared with using only a 25 kW diesel generator, the COE reduced from $0.373/kWh (using only DG/BS) to $0.337/kWh (using the best option) by around 9.65%. Under this condition, the values for the internal rate of return, return on investment, and simple payback are 11%, 7.8%, and 8.3 years, respectively.

1. Introduction

Fresh water is necessary for human existence and contemporary cultural advancement. Unfortunately, a sizable section of the world's population still does not have proper access to it [1, 2]. It is essential to have access to clean and safe water to sustain good hygiene, sanitation, and general health. There have been initiatives in recent years to solve this problem and increase access to fresh water globally. Numerous organizations, governments, and communities have collaborated to adopt sustainable water management practices, invest in infrastructure development, and promote water conservation measures. Desalination facilities, rainwater collection systems, and more effective irrigation practices are just a few examples of the alternative options being developed to boost the availability of fresh water. With the help of these programs, communities that lack adequate water resources will be given access to them [3, 4].

The literature has introduced several different water desalination techniques. With solar distillation, water is heated to produce evaporation, which is then condensed to make fresh water. Although it is a straightforward and affordable approach, its ability to produce vast amounts of water might be slow and limited [5]. Vacuum distillation: this process works with less pressure, enabling water evaporation to occur at lower temperatures. It is energy-efficient compared to other thermal distillation methods but still relatively expensive [6]. Multistage flash distillation (MSF) is the process of heating seawater under intense pressure until it flashes into steam. After that, the steam is condensed to create fresh water. Although it has been used extensively and is effective, this method uses a lot of energy. Multiple-effect distillation (MED): MED employs decreasingly pressurized evaporating and condensing chambers. Each subsequent chamber utilizes the energy released during condensation in the preceding chamber. Although MED is energy-efficient, its implementation can take time and effort [7]. Reverse osmosis (RO) is a widely used technique for removing salt and contaminants from water by passing a semipermeable membrane. High-pressure pumps are necessary to push the saline water through the membrane. RO is often employed in desalination facilities despite being energy-intensive and capable of great efficiency [8]. Membrane distillation: using a hydrophobic membrane, this technique separates water vapor from brackish or salty water. Compared to other distillation techniques, it operates at lower temperatures and pressures and can use low-grade heat sources. Membrane distillation has the potential to be an effective substitute. Each desalination approach has pros and cons, and things like the kind of water source, cost, size of operation, and energy availability influence the choice of method. Water desalination methods are continually being researched and developed to increase effectiveness, lower prices, and access to fresh water for people lacking it [9].

Traditional energy sources like coal and oil have several negative environmental consequences [10–12]. The release of greenhouse gases like carbon dioxide has influenced environmental problems and climate change. Additionally, local ecosystems may suffer grave consequences due to the extraction and exploitation of these resources. Thankfully, there has been an increase in the use of renewable energies. These sources have a far smaller negative environmental impact and do not emit greenhouse gases when in operation. They also have the advantage of being renewable so that they will not run out, unlike conventional resources. Although building infrastructure for renewable energy can initially be expensive, technological developments and economies of scale have slowly reduced the overall cost of producing clean energy [13].

Wind energy is a nontraditional energy source with enormous potential to help satisfy global energy needs [14]. Wind energy is a sustainable and ecofriendly solution because it is abundant, clean, and renewable. One of its major benefits is that wind energy does not emit any damaging pollutants or greenhouse gas emissions when generating power. As a result, it plays a key role in combating climate change and enhancing air quality. Additionally, wind is a resource abundantly found worldwide, making it a dependable and reachable energy source in many areas. Wind farms' efficiency and electricity output have significantly increased due to improvements in wind turbine technology and infrastructure. Because of this, wind energy is now more affordable than it once was, making it an attractive alternative to traditional fossil fuel-based energy sources [1+]. Therefore, due to the nature of wind, which does not depend on a specific time, wind energy can be generated at any time when the wind speed is enough to rotate wind turbines (unlike solar energy, which is only available during the day). For this reason, wind energy is considered the most reliable partner in any hybrid energy system [15–19].

Globally, as of 2022, around 77.6 GW of wind energy has been integrated into electrical grids, resulting in a cumulative installed capacity of 906 GW. Looking ahead, Africa and the Middle East are anticipated to introduce 17 GW of new capacities in the next five years (2023-2027), with specific projections including 5.3 GW in South Africa, 3.6 GW in Egypt, 2.4 GW in Saudi Arabia, and 2.2 GW in Morocco [20]. Kingdom of Saudi Arabia Vision 2030 works toward utilizing renewable energy sources (RES) to afford 9.5 GW of RES to avoid CO_2 emissions and to reduce dependence on the huge demand of fossil fuels for electricity production, industrialization, desalination, and transportation [21]. The King Abdullah City for Atomic and Renewable Energy (KACARE) schedules to employ a stable mix of viable atomic and feasible RES in a sustainable mode to generate energy and maintain the KSA's resources of natural gas and oil for future use. The generation of electricity in Saudi Arabia (SA) depends upon gas and oil capitals, and up to 240 terawatt-hours (TWh) of electricity is exhausted. 80% of electricity production is employed for air-conditioning (AC) needs. More than 17 million kWh is consumed by water distillation plants to afford around 235 L/day of drinking water per person. The major purpose for the expansion of a wide range of energy strategies is the decrease of energy security and cost. Hence, adopting an alternative energy plan in SA will create many jobs with a driving force for achieving the targets of sustainable development [22]. However, SA is very rich in RES such as hydropower, wind, solar photovoltaic

(PV), concentrating solar power (CSP), and biomass energy sources. The objective of KACARE is to increase the extension of nuclear and RES projects. Therefore, the KACARE planned by 2040 for extra employment of wind, nuclear, PV, and CSP with capacities of 9, 17.6, 16, and 25 GW, respectively [23].

Water is one of the most important elements of life in the universe. It also represents about 70% of the Earth's area. In addition, saltwater covers about 97.5% of the total water on the earth's surface [24]. Despite the large percentage covered by water from the surface of the earth, the rate of water demand is constantly increasing due to the increase in the population around the world and the uncontrolled consumption rate in heavy industries that depend on water in their production [25]. Saudi Arabia is considered one of the largest countries in water consumption rates in the world because it has no running water sources on its surface and because of the continuous increase in demand for water to increase the number of people and various industries.

In this regard and according to Qatrah, a program launched by the Saudi Arabian government to reduce water consumption, Saudi Arabia in 2019 had the 3rd highest water consumption rate per capita in the world. The average person in Saudi Arabia consumes around 263 L daily [26]. Qatrah program is aimed at reducing that amount to 150 L by 2030. On top of that, Saudi Arabia is one of the most water-scarce countries around the globe. These numbers should raise awareness of moderate water consumption, along with the importance of water production. Since the terrain of Saudi Arabia lacks rivers and lakes, the only source to acquire potable water is through desalination [27]. Desalinating enough water for around 35 million people requires massive energy consumption, and if fossil fuel is used, serious damage to the environment is expected [27].

With the scarcity of fresh drinking water and the increase in the demand for it, engineers around the globe came up with several techniques to desalinate water to keep up with that ever-increasing demand [28]. There are two types of water to desalinate: brackish water and seawater. The main difference between them is the degree of contaminants and the level of salts and minerals. Those impurities are higher in seawater. Since seawater is highly likely to contain impurities, it usually requires a pretreatment process. Usually, the seawater is taken to the plant from the surface of the sea, where the contaminants are more concentrated [24]. Drawing water from the surface also presents considerable damage to marine life and raises concerns about endangering some species. For that matter, subsurface water intake is a better alternative. By drilling a well in a location close to the shore, water reservoirs are accessed. This method, although unfavourable geologically, is less harmful to marine life. Also, the extracted water does not require as much pretreatment as the surface water.

The target of Qatrah project is to research the most suitable desalination technique for Saudi Arabia, and if it is economically achievable, implement as much renewable energy as possible [27]. In 2018, 17.1% of the world's energy generation came from renewable energy. Hydroelectric energy alone is responsible for 30% of the generated energy, while solar and wind energies contribute only 5% and 10%, respectively. Given the climate of Saudi Arabia, solar systems are the most suitable option currently. This is due to the high ground reflectance and the clear sky for almost the entire day [28]. Thus, a study on renewable energy and cost minimization will be conducted.

The target of this paper is to determine the optimal size of wind turbines (WT)/diesel generator (DG)/battery storage (BS) systems. The suggested WT/DG/BS system is implemented to feed seawater reverse osmosis (SWRO) unit in NEOM city as a case study. The targeted desalinated water per day is 100 m^3. Two main metrics are used to identify the optimal size of the WT/DG/BS system: minimum cost of energy (COE) and net present cost (NPC). For sensitivity analysis, two different ratings of the SWRO units (SWRO-100 and SWRO-150), three control dispatch strategies (load following, cycle charging, and combined dispatch), and five types of batteries are taken into consideration.

2. Location and Load Profile

NEOM city is located at latitude 29° 08′ and longitude 34° 55′ in Saudi Arabia. Figure 1 shows the average wind speed every month. The maximum wind speed of 6.68 m/s occurs in June followed by 6.11 m/s in September whereas the lowest wind speed of 5.04 m/s occurs in November [29]. The required electrical power is mainly used to feed a seawater reverse osmosis (SWRO) unit. The total desalinated water per day is 100 m^3. Table 1 presents the specifications of SWRO units. Considering Table 1, two SWRO units are considered for the case study: SWRO-100 and SWRO-150. In the case of using SWRO-100 to produce 100 per/day, SWRO-100 is required to operate at full capacity (24 hours per day). Consequently, the total consumed electrical energy is 600 kWh per day with a maximum of 25 kW. In the case of using SWRO-150 to produce 100 per/day, SWRO-150 is required to operate at 66.67% of full capacity (16 hours per day). Consequently, the total consumed electrical energy is 568 kWh per day with a maximum of 35.5 kW [30].

3. System Description

The schematic diagram of the WT/DG/BS system is demonstrated in Figure 2. The system contains a wind turbine (WT), diesel generator (DG), battery energy storage, and converter. It has been used to provide power to a certain load demand in NEOM city. The amount of wind energy available and the battery's level of charge influence the power flow in a wind turbine-battery-diesel generator combination. The wind turbine turns wind kinetic energy into electrical energy by capturing it. The turbine's blades rotate and power a generator to create electricity when the wind blows. A battery can be charged using the wind turbine's electrical output. When the wind is strong but not immediately needed, extra energy can be stored using the battery, which serves as a storage device. When the wind is not strong enough or when there is a great demand, the stored energy can then be utilized. A diesel generator can be utilized as a backup power source when the wind is not strong

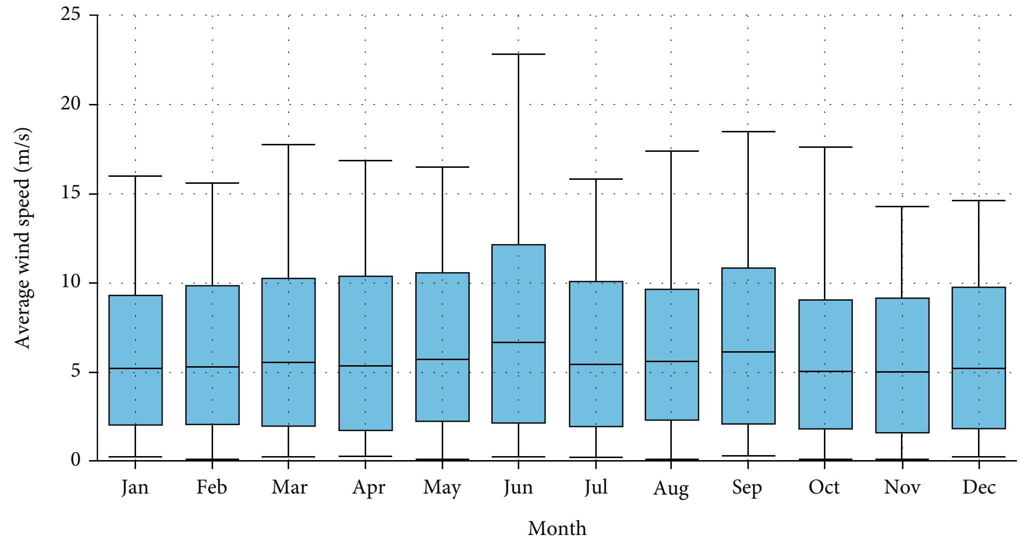

FIGURE 1: Average wind speeds every month.

TABLE 1: Specification of SWRO units.

Parameter	Unit	SWRO-50	SWRO-100	SWRO-150	SWRO-250
Permeate flow rate	m^3/day	50	100	150	250
Permeate recovery flow rate	$	40			
Raw water TDS	mg/L	<40			
Permeate water TDS	mg/L	<500			
Raw water TSS	mg/L	<30			
Power supply		AC 380, 3 phase, 50/60 Hz			
Power consumption	kW	20	25	35.5	52.5

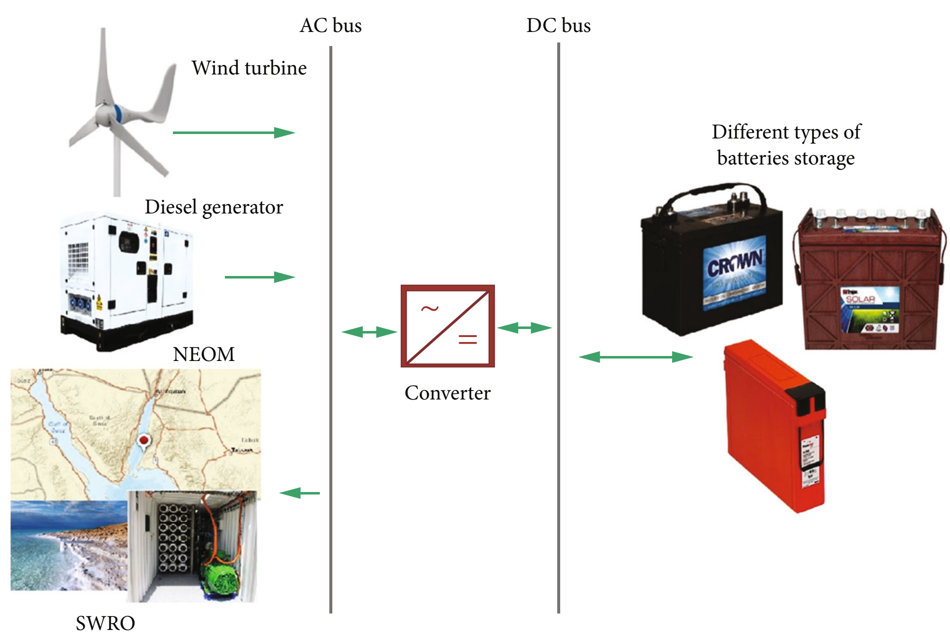

FIGURE 2: Schematic diagram of the WT/DG/BS system.

enough to generate enough electricity or when the battery is running low. The diesel generator generates electricity by burning fuel, typically diesel, and powering a generator. This system's power flow can be summed up as follows: the wind turbine generates electricity when the wind is strong enough, which can be utilized to directly power electrical loads or to recharge the batteries. The battery can be used to store extra electricity produced by the wind turbine during times of low demand or powerful gusts. The battery can deliver the stored energy to power the electrical loads when the wind is not strong enough or when the demand exceeds the output of the wind turbine. The diesel generator covers the extra power needed if the battery is low and there is a strong electricity demand. Overall, this system enables stable backup power from the diesel generator when required, efficient utilization of wind energy, and storage of excess energy.

3.1. Wind Turbine. The wind speed can be estimated at the height of the hub using the location wind speed employing the logarithmic laws as presented in the following relation [31].

$$V_{\text{hub}}(t) = V_{\text{ref}}(t) \times \left(\frac{H_{\text{hub}}}{H_{\text{ref}}}\right)^{\alpha}, \tag{1}$$

where, H_{ref} and H_{hub} denote the reference and hub height values, V_{ref} and V_{hub} denote the reference and hub speed values, and α is the ground roughness coefficient.

The WT output power can be represented and demonstrated by the following relation [31].

$$P_{\text{WT}} = \left\{ \begin{array}{c} 0, V_{\text{hub}} < V_{\text{cut-in}} V_{\text{hub}} < V_{\text{cut-out}} \\ V_{\text{hub}}^3(t)\left(\frac{P_r}{V_r^3 - V_{\text{cut-in}}^3}\right) - P_r\left(\frac{V_{\text{cut-in}}^3}{V_r^3 - V_{\text{cut-out}}^3}\right), V_{\text{cut-in}} \le V_{\text{hub}} \le V_r \\ P_r, V_r \le V_{\text{hub}} \le V_{\text{cut-out}} \end{array} \right\}, \tag{2}$$

where $V_{\text{cut-in}}$, $V_{\text{cut-out}}$, V_{r}, and P_{r} are the cut-in, cut-out, rated speed, and rated power of the wind turbine, respectively.

The yearly WT-produced energy can be estimated using the following relation.

$$E_{\text{WT}}(t) = N_{\text{WT}} \times P_{\text{WT}}(t) \times \Delta t, \tag{3}$$

where N_{WT} and Δt are the number of WTs and the time step of a simulation.

The participation of the renewable energy (f_{ren}) as apart from the total energy consumption of the system (E_{cons}) is expressed by the following:

$$f_{\text{ren}} = 1 - \frac{E_{\text{nonren}}}{E_{\text{cons}}}. \tag{4}$$

3.2. Diesel Generator. The produced AC power of a diesel generator (P_{DG}) is generated based on fuel consumption (F). The F is estimated to generate electricity by the following formula [32]:

$$F = A_1 \cdot C_{\text{DG}} + A_2 \cdot P_{\text{DG}}, \tag{5}$$

where A_1 and A_2 are the coefficient and slope of the fuel curves, consequently. The A_2 value is illustrated in Ref. [32]. The C_{DG} is DG capacity. The DG system net present cost (NPC_{DG}) can be evaluated including 4 main parameters that are the capital cost (C_{DG}), cost of operation and maintenance ($C_{\text{O\&M,DG}}$), cost of position ($C_{\text{P,DG}}$), and the cost of fuel (F). They can be formulated as the following expressions:

$$NPC_{DG} = C_{DG} + C_{O\&M,DG} + C_{P,DG} + \text{F}, \tag{6}$$

$$C_{\text{DG}} = \eta_{\text{DG}} \cdot P_{\text{DG}}, \tag{7}$$

$$C_{\text{O\&M,DG}} = t_{\text{run}} \cdot \sum_{i=1}^{n} \left(\frac{1-\beta}{1+r}\right)^{i}. \tag{8}$$

Table 2 shows the specifications of WT and DG.

3.3. Battery Storage. Different types of battery storage are considered as presented in Table 3. The battery power can be estimated using the following equation:

$$P_B = P_{B-i} + \int_0^t V_B \cdot I_B \cdot dt, \tag{9}$$

where P_{B-i} is the battery power at starting, V_B is the voltage, and I_B denoted the current.

The set-point state of charge (SOC_B) is the ratio of Eq. (9) to the maximum charge of the battery ($P_{B,\max}$) as follows [33]:

$$\text{SOC}_B = \frac{P_B}{P_{B,\max}} \times 100(\%). \tag{10}$$

As explained in the following relation, the battery capacity C_B is represented in terms of load demand (P_L), discharge depth (D_d), battery autonomy/day (A_d), and battery and converter efficiencies η_B and η_C, consequently.

$$C_B = \frac{(\text{P}_{\text{L}} \times \text{A}_{\text{d}})}{(\eta_B \times \eta_C \times D_d)}. \tag{11}$$

3.4. Control Strategies. Controlling a system is very important in any project. When any proposed system has a qualified control strategy, many advantages and specifications will be ensured such as minimizing the cost, high performance, and stable system. However, the controller of the energy management strategy (EMS) is responsible for making a comprehensive analysis of the produced power of WT with the load power to estimate the flow of energy. In the case of the generated power from WT being higher than the load power, the batteries will be charged by the excessing power if the set-point state of charge is not attaining the maximum set-point. Moreover, in the case of the generated power from WT being higher than the load power and the batteries not attaining the minimum set-point, batteries can supply the load (discharge process). On the other hand, in the case of the batteries attaining the minimum set-point, the diesel generator starts producing its power to supply the load. In this

Table 2: Specifications of WT and DG.

Component	Specifications
Wind turbine	Name: Ecoycle EXO-M-26 Capacity range: 90 kW Manufacture: Ecoycle Rotor diameter: 25 m Hub height: 32 m Speed: cut-in is 2.75 m/s; cut-out is 20 m/s Initial cost is $180,000, replacement is $180,000, and O&M is $9,000/year Lifespan: 30 years
Diesel generator (kW)	Rating: 25 kW Fuel: density is 820 kg/m^3, lower heating value is 43.2 MJ/kg, and fuel consumption is 0.273 L/h/kW Initial cost is $500/kW, replacement is $500/kW, and O&M is $0.7/hour Lifespan: 15000 hours
Converter (kW)	Initial cost is $300/kW, replacement is $300/kW, and O&M is $5/year Lifespan: 15 years Efficiency: 95%
Control strategies	Load following, cycle charging, and combined strategy

Table 3: Technical battery data.

Name	EnerSys PowerSafe SBS 190F	CROWN 12CRV100 AGM	Fortress Power eVault LFP-15	Surrette S-260	Trojan SAGM 12 205
Nominal voltage (V)	12	12	48	12	12
Nominal capacity (kWh)	2.57	1.28	14.4	3.12	2.63
Maximum capacity (Ah)	214	107	330	260	319
Capacity ratio	0.489	0.515	0.4	0.361	0.039
Roundtrip efficiency (%)	97	80	98	80	85
Maximum charge current (A)	190	30	130	80	41
Maximum discharge current (A)	983		150	80	300
Maximum charge rate (A/Ah)	1	1	1	0.379	1
Capital cost ($/unit)	900	400	10500	350	465
Initial SOC (%)	100	100	100	100	100
Minimum SOC (%)	30	40	5	40	20
Throughout (kWh)	27,47.70	350	60,000	1,704.9	2,285.10
Time (years)	15.0	10	10	12	

regard, three control strategies are considered load following (LF), cycle charging (CC) and combined dispatch CD).

3.4.1. Load Following Strategy. The load following strategy produces the power to meet the primary load only when the generator is operated. Under the load following strategy, there are three cases [34]:

(i) The first case is when the demand of the load meets the WT power. In this case, there is no energy in the batteries, so the generator will be off. In addition, the load power will be equal to WT output power, and there is no excess power

(ii) The second case happens when the load power is lower than the WT output power. However, if the battery is fully charged, the excess power will be damped. The WT excess power is used to charge the battery only if the battery is not fully charged. So, the generator will be off

(iii) The third case happened when the load power was higher than the WT power. The DG produces only enough power to meet the primary load

3.4.2. Cycle Charging Strategy. The cycle charging strategy is the same as the load following strategy, and both are dispatch strategies, but they differ from each other when the DG is switched on, the net load will be at the maximum rated capacity, and the battery will be charged with excess power [34].

Table 4: Optimal results of the WT/DG/BS system considering thirteen different options.

Options	EMS	RO	No. WT	DG kW	No. BS	Converter kW	NPC ($)	COE ($/kWh)	O&M cost ($/y)	Initial cost ($)	Fuel (L/yr)	Autonomy (hr)	Throughout (kWh/yr)
CROWN 12CRV100 battery													
1	CC	100	1	25	27	16.6	1.01 M	0.356	61,907	208,276	43,183	0.831	472
2	CD	100	1	25	5	2.61	991,029	0.35	61,554	195,284	43,475	.154	133
3	LF	100	1	25	27	16.6	1.01 M	0.356	61,850	208,281	43,136	0.831	500
4	CC	150	1	25	295	32.4	1.73	0.646	109,040	320,221	41,366	9.59	45,157
5	CD	150	2	25	412	42.8	1.85	0.689	100,285	550,139	28,283	13.4	44,929
6	LF	150	2	25	417	37.9	1.85 M	0.689	100,201	550,681	28,174	13.6	45,069
PowerSafe SBS XC 190F													
7	CC	100	1	25	15	19.4	991,199	0.35	60,287	211,833	42,361	1.05	3243
8	CD	100	1	25	12	9.12	976,393	0.345	59,590	206,036	41,637	0.842	4,084
9	LF	100	1	25	19	19.9	985,306	0.348	59,543	215,565	41,161	1.33	4,126
10	CC	150	1	25	109	34.4	1.18 M	0.44	67,870	300,909	39,175	8.08	43,281
11	CD	150	2	25	162	34	1.31 M	0.489	60,401	528,495	27,892	12	41,475
12	LF	150	2	25	162	34	1.31 M	0.489	60,422	528,495	27,907	12	41,463
eVault LFP-15													
13	CC	100	1	25	3	15.7	1.05 M	0.371	63,453	228,700	43,535	1.64	160
14	CD	100	1	25	1	6.76	984,795	0.348	60,319	205,027	42,445	0.547	2,116
15	LF	100	3	25	67	95.8	2.17 M	0.766	68,404	1.28 M	835	36.7	139,605
16	CC	150	1	25	15	31.3	1.22 M	0.454	66,259	359,402	39,865	8.67	47,541
17	CD	150	2	25	22	28.7	1.44 M	0.537	63,952	612,114	27,907	12.7	41,258
18	LF	150	2	25	77	96	2.34 M	0.875	73,852	1.39 M	184	44.5	136,919
SurrS-260													
19	CC	100	1	25	37	20.5	979,605	0.346	59,409	211,593	41,530	2.77	6,041
20	CD	100	1	25	24	10.1	966,063	0.341	58,953	203,942	41,184	1.8	5,984
21	LF	100	3	25	715	101	1.55 M	0.547	55,378	833,163	842	53.6	154,467
22	CC	150	1	25	187	25.4	1.12 M	0.419	66,258	265,572	40,428	14.8	47,225
23	CD	150	4	25	578	102	1.78 M	0.665	63,179	965,479	329	45.8	150,924
24	LF	150	4	25	591	111	1.79 M	0.668	63,180	972,622	196	46.8	151,460
Trojan SAGM 12 205													
25	CC	100	1	25	29	20	981,568	0.347	59,531	211,977	41,838	2.44	4,924
26	CD	100	1	25	47	23.8	950,725	0.337	56,409	221,495	36,396	3.95	23,017
27	LF	100	3	25	538	99.4	1.51 M	0.533	52,292	832,477	866	45.2	149,800
28	CC	150	1	25	173	26.8	1.11 M	0.413	63,958	281,000	39,340	15.4	47,104
29	CD	150	3	25	172	24.5	1.49 M	0.557	66,001	639,820	27,892	15.3	43,681
30	LF	150	3	25	584	106	1.51 M	0.564	50,710	855,874	183	51.9	146,991

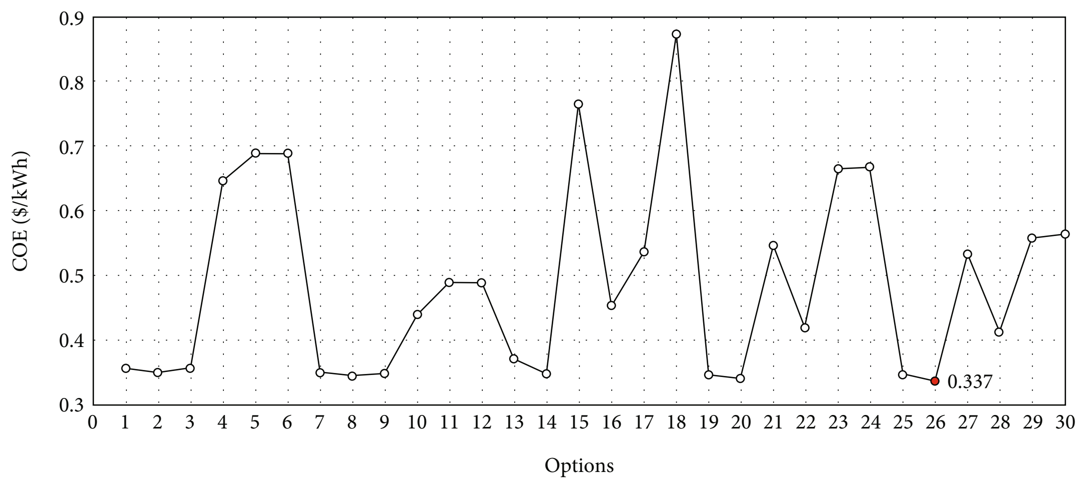

Figure 3: Values of COE considering thirteen different options.

Table 5: Cost summary for the best option.

Component	Capital ($)	Replacement ($)	O&M ($)	Fuel ($)	Salvage ($)	Total ($)
WT	180,000.00	0.00	116,347.65	0.00	7,186.74	289,160.91
DG	12,500.00	45,560.12	46,451.80	471,311.70	44.92	575,778.70
Converter	7,127.59	3,024.05	0.00	0.00	569.16	9,582.48
BS	22,320.00	53,457.80	6,205.21	0.00	3,690.25	78,292.76
System	221,947.59	102,041.96	169,004.66	471,311.70	11,491.06	952,814.85

3.4.3. Combined Dispatch Strategy. A combined dispatch strategy is a combination of the cycle charging strategy and load following strategy. This strategy may allow the system to be more efficient for the generator and battery [35]. In this strategy, the future net load will be investigating whether the generator to charge the battery or not [35]. If the net load is low, this strategy will use the cycle charging strategy, and if the net load is high, this strategy will use the load following strategy. According to the combined dispatch strategy, it ensures that the system produces a high performance in terms of energy access better than cycle charging and load following individually.

Considering the combined dispatch strategy, there are three case scenarios to obtain the best choice for the lowest cost as follows:

(i) The first case is when the battery is not charged when the generator generates only electricity to get the net load

(ii) The second case happened when the battery is charged and allowed the excess power if the generator provided the net load requirements

(iii) The last case happened when only the battery supplied the net load

4. Evaluation Criterion and Limitations

4.1. Evaluation Criterion. The optimal size of the WT/DG/BS is determined based on the minimum NPC "net present cost" and the minimum COE "cost of energy" [29]. The NPC can be estimated using the following relation.

$$\mathrm{NPC} = \frac{C_{\mathrm{ann,tot}}}{\mathrm{CRF}_{(i,N)}}, \tag{12}$$

where $C_{\mathrm{ann,tot}}$ is the annual cost, i is the real interest rate (6%), N is the project lifespan "25 years", and CRF is the capital recovery factor as follows:

$$\mathrm{CRF}(i, N) = \frac{i(1+i)^N}{(1+i)-1}. \tag{13}$$

The total annual cost $C_{\mathrm{ann,tot}}$ considers initial cost, O&M costs that are typically for the WT. In the case of the battery and the inverter, the replacement cost will be added.

SV "salvage value" can be determined as follows:

$$\mathrm{SV} = C_{\mathrm{rep}} \frac{R_{\mathrm{rem}}}{R_{\mathrm{comp}}}, \tag{14}$$

where C_{rep} is the components' replacement cost, R_{rem} is the rest of the lifetime, and R_{comp} is the lifetime.

The COE can be estimated using the following relation.

$$COE = \frac{C_{\mathrm{ann,tot}}}{E_{\mathrm{prim}} + E_{\mathrm{def}} + E_{\mathrm{grid,sales}}}, \tag{15}$$

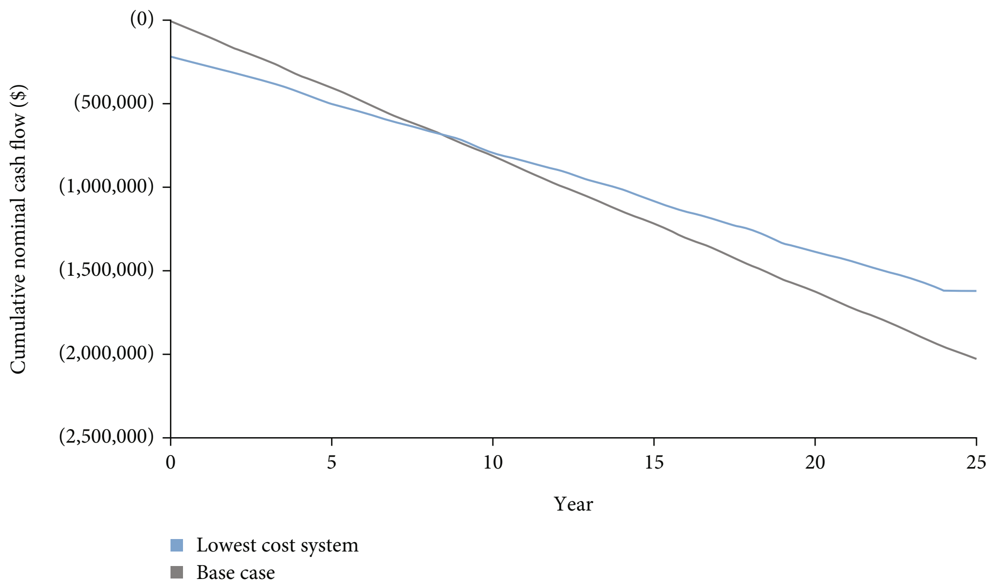

Figure 4: Cumulative nominal cash flow.

Table 6: Economic comparison between the best option and the base system.

	Nominal cash flows				Discounted cash flows			
	Best option		Base system (DG/BS)		Best option		Base system (DG/BS)	
Year	Annual	cumulative	Annual	cumulative	Annual	cumulative	Annual	cumulative
0	221,947.59	221,947.59	14,726.25	14,726.25	221,947.59	221,947.59	14,726.25	14,726.25
1	49,531.27	271,478.86	73,614.00	88,340.25	46,779.54	268,727.12	69,524.33	84,250.58
2	49,531.27	321,010.14	86,114.00	174,454.25	44,180.67	312,907.80	76,996.41	161,246.99
3	49,531.27	370,541.41	73,614.00	248,068.25	41,726.19	354,633.99	62,013.99	223,260.98
4	62,031.27	432,572.68	86,114.00	334,182.25	49,859.86	404,493.85	68,846.51	292,107.49
5	71,851.27	504,423.96	73,614.00	407,796.25	54,272.44	458,766.28	55,314.95	347,422.44
6	49,531.27	553,955.23	86,114.00	493,910.25	35,151.02	493,917.31	61,561.37	408,983.81
7	62,031.27	615,986.50	86,114.00	580,024.25	41,937.38	535,854.69	57,790.13	466,773.94
8	49,531.27	665,517.78	73,614.00	653,638.25	31,353.85	567,208.53	46,598.48	513,372.42
9	49,531.27	715,049.05	86,114.00	739,752.25	29,611.97	596,820.50	51,672.33	565,044.75
10	84,351.27	799,400.32	73,614.00	813,366.25	48,304.04	645,124.54	41,564.69	606,609.44
11	49,531.27	848,931.60	86,114.00	899,480.25	26,413.14	671,537.68	46,203.76	652,813.20
12	49,531.27	898,462.87	86,114.00	985,594.25	24,945.75	696,483.42	43,375.06	696,188.26
13	62,031.27	960,494.14	73,614.00	1,059,208.25	29,669.75	726,153.17	35,014.98	731,203.24
14	49,531.27	1,010,025.42	86,114.00	1,145,322.25	22,250.99	748,404.16	38,782.66	769,985.89
15	78,978.86	1,089,004.28	74,445.25	1,219,767.50	33,994.48	782,398.64	31,585.17	801,571.07
16	62,031.27	1,151,035.55	86,114.00	1,305,881.50	24,956.06	807,354.70	34,677.65	836,248.72
17	49,531.27	1,200,566.83	73,614.00	1,379,495.50	18,744.70	826,099.41	27,858.61	864,107.33
18	49,531.27	1,250,098.10	86,114.00	1,465,609.50	17,703.33	843,802.74	31,008.22	895,115.55
19	84,351.27	1,334,449.37	86,114.00	1,551,723.50	28,598.07	872,400.81	29,108.54	924,224.09
20	49,531.27	1,383,980.65	73,614.00	1,625,337.50	15,790.93	888,191.75	23,468.68	947,692.77
21	49,531.27	1,433,511.92	86,114.00	1,711,451.50	14,913.66	903,105.41	26,027.08	973,719.85
22	62,031.27	1,495,543.19	73,614.00	1,785,065.50	17,656.82	920,762.22	20,933.49	994,653.34
23	49,531.27	1,545,074.47	86,114.00	1,871,179.50	13,302.62	934,064.84	23,272.63	1,017,925.97
24	71,851.27	1,616,925.74	86,114.00	1,957,293.50	18,375.47	952,440.30	21,847.74	1,039,773.71
25	1,563.48)	1,618,489.22	66,941.92	2,024,235.42	374.54	952,814.85	16,036.46	1,055,810.17

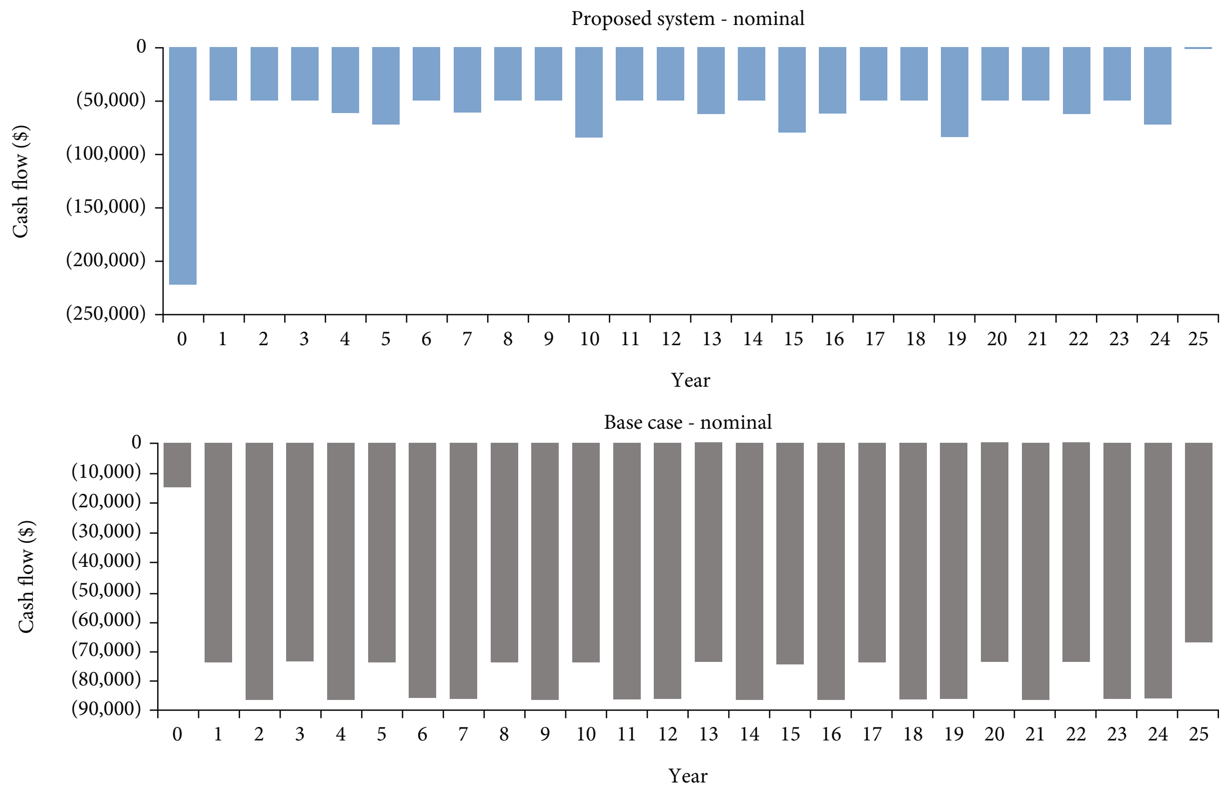

Figure 5: Cash flow for both the best option and the base system.

where E_{prim} is the primary energy sold to the grid, E_{def} is the deferrable energy sold to the grid, and $E_{grid,sales}$ is the electrical energy sold to the grid.

4.2. Limitations and Constrains. The main objective of the optimization process in this work is minimizing the cost of energy. The limitations and constrains of this research work can be outlined as follows.

(i) Only two sizes of RO are considered

(ii) Only one size of DG is considered

(iii) Number of wind turbines is integer and subject to $0 \leq N_{wind} \leq N_{wind}^{max}$

(iv) Number of batteries is integer and subject to $0 \leq N_{batt} \leq N_{batt}^{max}$

5. Results and Discussion

In the case study, to identify the optimal size of WT/DG/BS to supply a certain load in NEOM city, thirteen different options including five different batteries, two sizes of SERO units, and three energy management strategies are considered. HOMER software is applied to do the optimization process and identify the best option based on the minimum cost of energy. The optimized results considering thirteen different options are demonstrated in Table 4. In the case of using CROWN 12CRV100 battery, the COE ranged between \$0.35/kWh and \$0.689/kWh. The lowest COE of \$0.35/kWh is obtained when using the combined control strategy and SWRO-100 unit, whereas the worst COE of \$0.689/kWh is obtained when using load following control strategy and SWRO-150 unit. In the case of using PowerSafe SBS XC 190F battery, the COE ranged between \$0.345/kWh and \$0.489/kWh. The lowest COE of \$0.345/kWh is obtained when using the combined control strategy and SWRO-100 unit, whereas the worst COE of \$0.489/kWh is obtained when using load following control strategy and SWRO-150 unit. In sum, the best battery storage is Trojan SAGM battery. In this case, the COE ranged between \$0.337/kWh and \$0.564/kWh. The lowest COE of \$0.377/kWh is obtained when using the combined control strategy and SWRO-100 unit, whereas the worst COE of \$0.564/kWh is obtained when using load following control strategy and SWRO-150 unit. Figure 3 shows the values of COE considering thirteen different options.

The best option of the WT/DG/BS system to supply the SWRO unit is option number 26. This system includes one wind turbine of 90 kW, DG of 25 kW, 47 Trojan SAGM batteries, a 23.8 kW converter, a SWRO-100 unit, and the combined control strategy. The net present cost and the initial cost are \$950725 and \$221495, respectively. The annual operating cost and annual consumed fuel are \$56409 and 36396 L, respectively. Table 5 shows the cost summary for the best option.

Compared with using only a 25 kW diesel generator, the COE reduced from \$0.373/kWh (using only DG/BS) to \$0.337/kWh (using the best option) by around 9.65%. Under this condition, the values for internal rate of return (IRR) and return on investment (ROI) are 11% and 7.8%, respectively. Considering Figure 4, the cumulative nominal cash

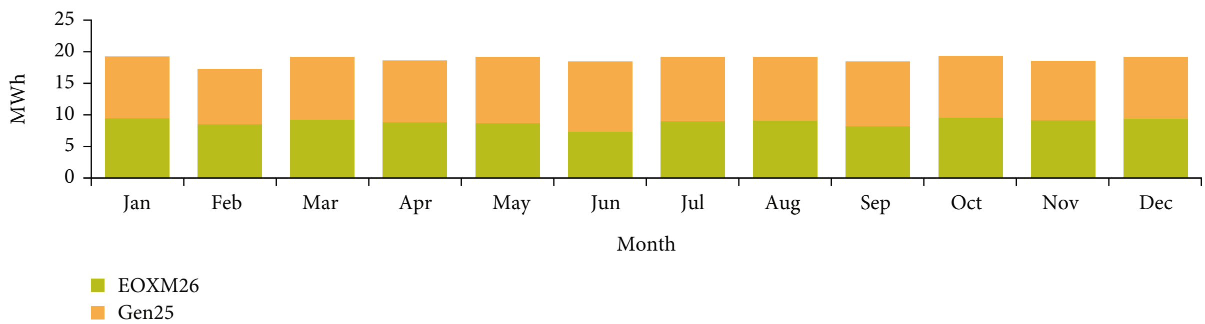

Figure 6: Monthly electric production by wind turbine and DG.

Figure 7: Electrical power daily profile by the wind turbine.

flow, the simple payback is 8.3 years. Table 6 shows the economic comparison between the best option and the base system. The cash flow for both the best option and base system is demonstrated in Figure 5.

The monthly electric production is presented in Figure 6. The total annual produced energy is 225,851 kWh. 47.3% (106,783 kWh) of the total annual energy is produced by WT and 52.7% (119,068 kWh) by DG. The total consumption per year is 218,196 kWh. In this case, the excess energy is around 0.653% (1,475 kWh), and the annual unmet load is 0.367% (804 kWh). Therefore, the annual capacity shortage is 0.0217% (47.4 kWh). The electrical power daily profile by wind turbine is demonstrated in Figure 7. The detailed output for different components of the WT/DG/BS system is presented in Table 7. Figure 8 shows the electrical power daily profile by DG.

Considering Table 6 and Figure 8, the mean electrical output power, minimum power, and maximum power are 24.9 kW, 6.25 kW, and 25 kW, respectively. The number of hours of operation of the DG is 479 hrs/yr whereas the number of starts is 992 starts/yr. The mean electrical efficiency is 33.2%.

The number of the required batteries is 48, and the expected life is 4.71 yr. The annual energy in and out are 25,255 kWh and 21,478 kWh, respectively, with annual storage depletion of 12 kWh. The total annual losses are 3,789 kWh. The state of charge daily profile of the battery is outlined in Figure 9.

Figure 10 presents a comparison study of the obtained COE for previous literature [36–39] and the present study. The comparison demonstrated the competitivity of the proposed configuration compared with other works.

Table 7: Detailed output for different components of the WT/DG/BS system.

Quantity	Value	Unit	Quantity	Value	Unit
Wind turbine					
Total rated capacity	90.0	kW	Maximum output	47.6	kW
Mean output	12.2	kW	Wind penetration	48.8	%
Capacity factor	13.5	%	Hours of operation	3,377	hrs/yr
Total production	106,783	kWh/yr	Levelized cost	0.209	$/kWh
Diesel generator					
Hours of operation	4,791	hrs/yr	Electrical production	119,068	kWh/yr
Number of starts	992	starts/yr	Mean electrical output	24.9	kW
Operational life	3.13	yr	Minimum electrical output	6.25	kW
Capacity factor	54.4	%	Maximum electrical output	25.0	kW
Fixed generation cost	2.41	$/hr	Specific fuel consumption	0.306	L/kWh
Marginal generation cost	0.273	$/kWh	Fuel energy input	358,747	kWh/yr
Fuel consumption	36,458	L	Mean electrical efficiency	33.2	%
Battery storage					
Autonomy	4.03	hr	Batteries	48.0	qty.
Storage wear cost	0.221	$/kWh	Energy in	25,255	kWh/yr
Nominal capacity	126	kWh	Energy out	21,478	kWh/yr
Usable nominal capacity	101	kWh	Storage depletion	12.0	kWh/yr
Lifetime throughput	109,685	kWh	Losses	3,789	kWh/yr
Expected life	4.71	yr	Annual throughput	23,296	kWh/yr
Converter					
Hours of operation	1,608	2,382	Energy in	21,478	26,585
Energy out	20,404	25,255	Losses	1,074	1,329

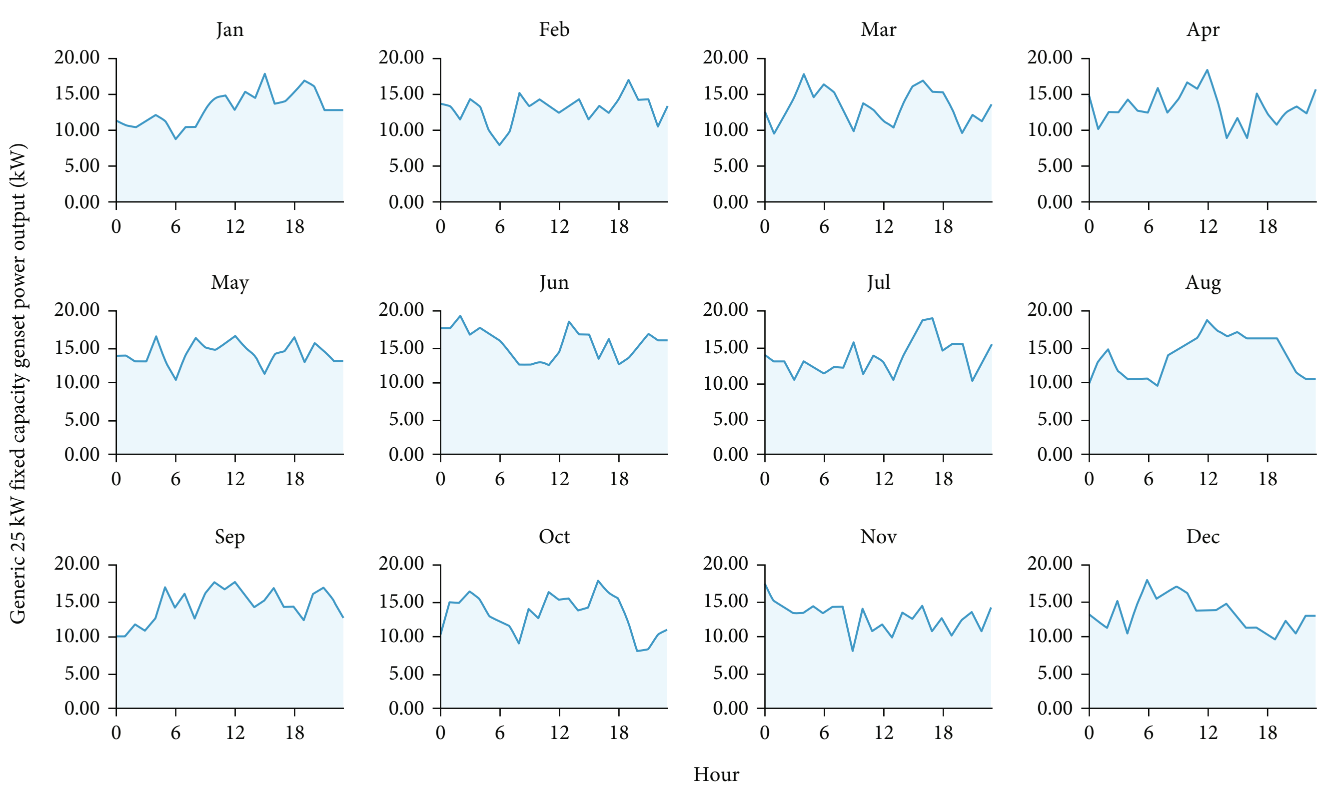

Figure 8: Electrical power daily profile by DG.

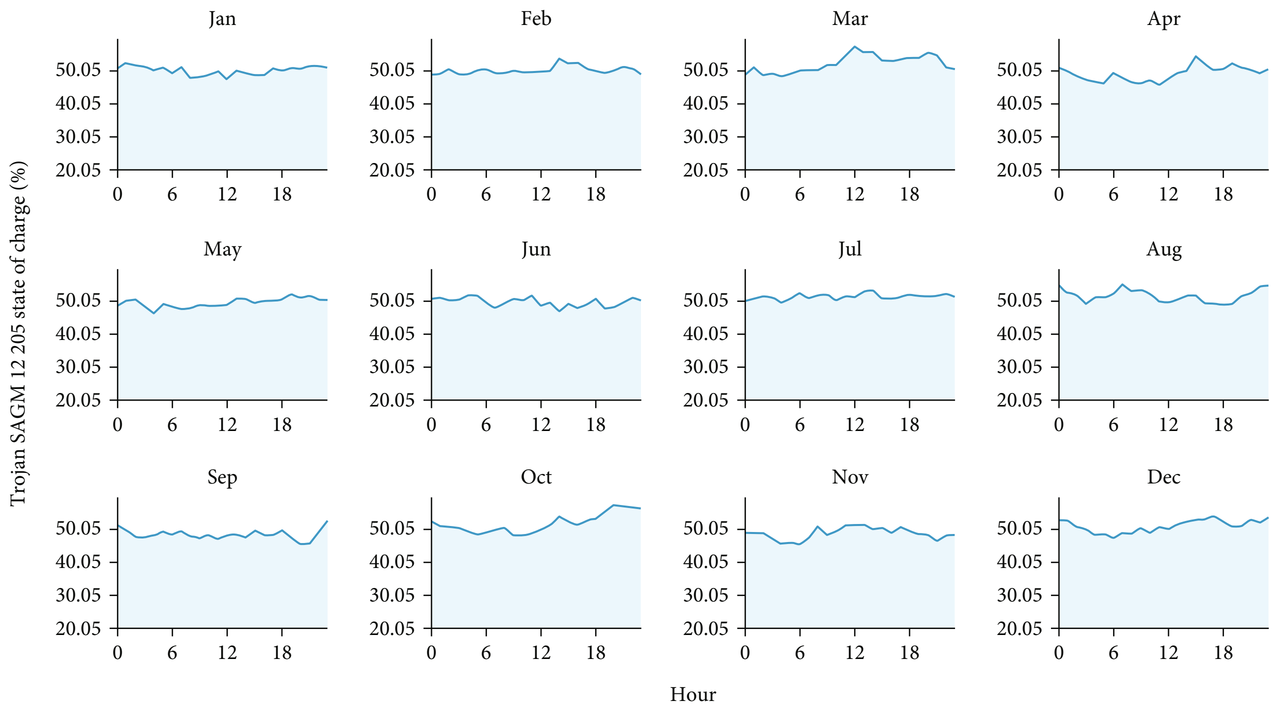

FIGURE 9: State of charge daily profile of the battery.

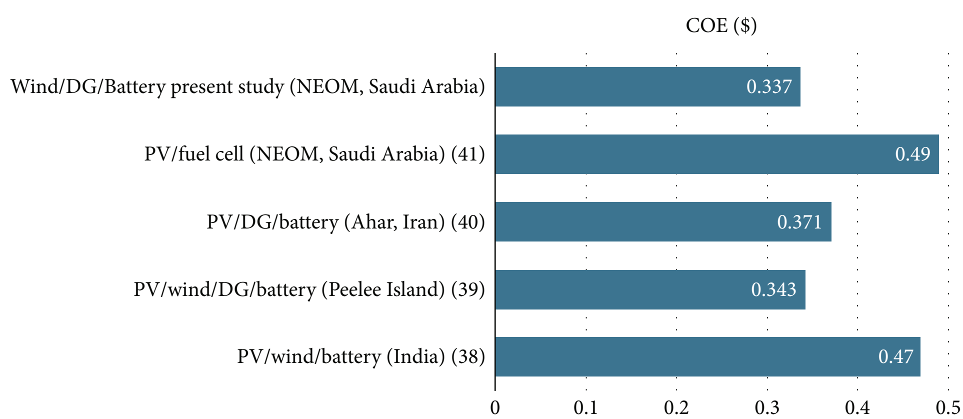

FIGURE 10: COE values for previous literature and the present study.

6. Conclusion

To power a seawater desalination unit in NEOM city, this article is aimed at establishing the ideal size of a wind turbine/diesel generator/battery storage (WT/DG/BS) system. The seawater desalination unit has a daily capacity of 100 m^3. Optimization was done using HOMER software at the lowest possible energy cost. To find out the best solution for the case study, five different battery types (Fortress Power eVault LFP-15, Surrette S-260, Trojan SAGM 12 205, EnerSys PowerSafe SBS 190F, and CROWN 12CRV100 AGM), two SWRO units (SWRO-100 and SWRO-150), and three control strategies (load following, cycle charging, and combined strategy) were all considered. According to the optimization results, the optimum battery storage is a Trojan SAGM battery. The COE in this instance varied from 0.337 to 0.564 dollars per kWh. The SWRO-100 unit and combined control strategy yield the lowest COE of $0.377/kWh. The SWRO-150 unit with load following the control approach provides the largest COE of $0.564/kWh. Option 26 is the WT/DG/BS system's best choice for supplying the SWRO unit. This system consists of a 90 kW wind turbine, a 25 kW diesel generator, 47 Trojan SAGM batteries, a 23.8 kW converter, an SWRO-100 unit, and a combined control scheme. Initial cost and net present cost are 950,725 and 221,495 dollars, respectively. The yearly running expenses and fuel consumption are 56,409 dollars and 36,396 liters, respectively. The COE decreased from $0.373/kWh (using only DG/BS) to $0.337/kWh (using the best option) by about 9.65% compared to a 25 kW diesel generator alone. Under this scenario, the internal rate of return, return on investment, and simple payback have values of 11%, 7.8%, and 8.3 years, respectively. Finally, regarding the cost of water production will be considered in the future work.

Data Availability

Data will be made available on request.

Conflicts of Interest

The authors declare no conflicts of interest.

Authors' Contributions

Mohamed K. Hassan and Hegazy Rezk were responsible for the conceptualization. Hegazy Rezk and Ayman Al-Quraan were responsible for the software. Hegazy Rezk, Hamdy Youssef, and Ahmed S. Shehata were responsible for the formal analysis. Hegazy Rezk and Alaa A. El-Bary were responsible for the investigation. Mohamed K. Hassan, Hegazy Rezk, and Ayman Al-Quraan wrote the original draft. Mohamed K. Hassan, Hegazy Rezk, Hamdy Youssef, Ahmed S. Shehata, Alaa A. El-Bary, and Ayman Al-Quraan wrote, reviewed, and edited the manuscript.

Acknowledgments

The authors extend their appreciation to the Deanship for Research & Innovation, Ministry of Education in Saudi Arabia, for funding this research work through the project number IFP22UQU4361238DSR078.

References

[1] Y. Aldali, K. Morad, N. Elminshawy, and F. Ahwide, "Numerical simulation of the integrated solar/hybrid desalination system," *Solar Energy and Sustainable Development Journal*, vol. 6, no. 2, pp. 42–54, 2017.

[2] M. Mallek, M. A. Elleuch, J. Euchi, and Y. Jerbi, "Optimum design of on-grid PV/wind hybrid system for desalination plant: a case study in Sfax, Tunisia," *Desalination*, vol. 576, article 117358, 2024.

[3] G. Kyriakarakos, A. I. Dounis, K. G. Arvanitis, and G. Papadakis, "Design of a fuzzy cognitive maps variable-load energy management system for autonomous PV-reverse osmosis desalination systems: a simulation survey," *Applied Energy*, vol. 187, pp. 575–584, 2017.

[4] E. Koutroulis and D. Kolokotsa, "Design optimization of desalination systems power-supplied by PV and W/G energy sources," *Desalination*, vol. 258, no. 1-3, pp. 171–181, 2010.

[5] A. G. Olabi, K. Obaideen, M. A. Abdelkareem et al., "Wind energy contribution to the sustainable development goals: case study on London array," *Sustainability*, vol. 15, no. 5, p. 4641, 2023.

[6] E. J. N. Baticados, S. C. Capareda, S. Liu, and M. Akbulut, "Advanced solar still development: improving distilled water recovery and purity via graphene-enhanced surface modifiers," *Frontiers in Environmental Science*, vol. 8, article 531049, 2020.

[7] W. L. Luyben, "Optimum vacuum distillation pressure," *Chemical Engineering and Processing-Process Intensification*, vol. 171, article 108630, 2022.

[8] A. J. Toth, "Modelling and optimisation of multi-stage flash distillation and reverse osmosis for desalination of saline process wastewater sources," *Membranes*, vol. 10, no. 10, p. 265, 2020.

[9] S. Aly, H. Manzoor, S. Simson, A. Abotaleb, J. Lawler, and A. N. Mabrouk, "Pilot testing of a novel multi effect distillation (MED) technology for seawater desalination," *Desalination*, vol. 519, article 115221, 2021.

[10] S. Sambhi, H. Sharma, V. Bhadoria et al., "Economic feasibility of a renewable integrated hybrid power generation system for a rural village of Ladakh," *Energies*, vol. 15, no. 23, p. 9126, 2022.

[11] C. Pavlatos, E. Makris, G. Fotis, V. Vita, and V. Mladenov, "Utilization of artificial neural networks for precise electrical load prediction," *Technologies*, vol. 11, no. 3, p. 70, 2023.

[12] M. A. Al-Obaidi, J. P. Li, C. Kara-Zaïtri, and I. M. Mujtaba, "Optimisation of reverse osmosis based wastewater treatment system for the removal of chlorophenol using genetic algorithms," *Chemical Engineering Journal*, vol. 316, pp. 91–100, 2017.

[13] S. Parani and O. Oluwafemi, "Membrane distillation: recent configurations, membrane surface engineering, and applications," *Membranes*, vol. 11, no. 12, p. 934, 2021.

[14] S. Mohammed, Y. Nassar, W. El-Osta, H. J. El-Khozondar, A. Miskeen, and A. Basha, "Carbon and energy life cycle analysis of wind energy industry in Libya," *Journal of Solar Energy and Sustainable Development*, vol. 12, no. 1, pp. 50–69, 2023.

[15] Y. F. Nassar, S. Y. Alsadi, H. J. El-Khozondar et al., "Design of an isolated renewable hybrid energy system: a case study," *Materials for Renewable and Sustainable Energy*, vol. 11, no. 3, pp. 225–240, 2022.

[16] Y. F. Nassar, M. J. Abdunnabi, M. N. Sbeta et al., "Dynamic analysis and sizing optimization of a pumped hydroelectric storage-integrated hybrid PV/wind system: a case study," *Energy Conversion and Management*, vol. 229, article 113744, 2021.

[17] Y. Nassar and S. Alsadi, "Economical and environmental feasibility of the renewable energy as a sustainable solution for the electricity crisis in the Gaza Strip," *International Journal of Engineering Research and Development*, vol. 12, no. 3, pp. 35–44, 2016.

[18] A. F. M. Ali, E. M. H. Karram, Y. F. Nassar, and A. A. Hafez, "Reliable and economic isolated renewable hybrid power system with pumped hydropower storage," in *2021 22nd International Middle East Power Systems Conference (MEPCON)*, pp. 515–520, Assiut, Egypt, December 2021.

[19] H. J. El-Khozondar, F. El-batta, R. J. El-Khozondar, Y. Nassar, M. Alramlawi, and S. Alsadi, "Standalone hybridPV/wind/diesel-electric generator system for a COVID-19 quarantine center," *Environmental Progress & Sustainable Energy*, vol. 42, no. 3, article e14049, 2023.

[20] Y. Nassar, A. Alatrash, B. Ahmed et al., "Assessing the viability of solar and wind energy technologies in semi-arid and arid regions: a case study of Libya's climatic conditions," *Applied Solar Energy*, vol. 1, 2024.

[21] S. K. Sahoo, "Renewable and sustainable energy reviews solar photovoltaic energy progress in India: a review," *Renewable and Sustainable Energy Reviews*, vol. 59, pp. 927–939, 2016.

[22] Y. A. Amran, Y. H. M. Amran, R. Alyousef, and H. Alabduljabbar, "Renewable and sustainable energy production in Saudi Arabia according to Saudi Vision 2030; current status and future prospects," *Journal of Cleaner Production*, vol. 247, article 119602, 2020.

[23] N. L. Panwar, S. C. Kaushik, and S. Kothari, "Role of renewable energy sources in environmental protection: a review," *Renewable and Sustainable Energy Reviews*, vol. 15, no. 3, pp. 1513–1524, 2011.

[24] M. Chandrashekara and A. Yadav, "Water desalination system using solar heat: a review," *Renewable and Sustainable Energy Reviews*, vol. 67, pp. 1308–1330, 2017.

[25] R. Ben-Mansour, A. H. Al-Jabr, and R. Saidur, "Economic comparison between RO-wind and RO-PV desalination systems," *Desalination and Water Treatment*, vol. 156, pp. 7–19, 2019.

[26] U. Caldera, D. Bogdanov, S. Afanasyeva, and C. Breyer, "Role of seawater desalination in the management of an integrated water and 100% renewable energy based power sector in Saudi Arabia," *Water*, vol. 10, no. 1, p. 3, 2018.

[27] A. M. Ghaithan, A. Al-Hanbali, A. Mohammed, A. M. Attia, H. Saleh, and O. Alsawafy, "Optimization of a solar-wind-grid powered desalination system in Saudi Arabia," *Renewable Energy*, vol. 178, pp. 295–306, 2021.

[28] S. Mandal, B. K. Das, and N. Hoque, "Optimum sizing of a stand-alone hybrid energy system for rural electrification in Bangladesh," *Journal of Cleaner Production*, vol. 200, pp. 12–27, 2018.

[29] https://www.homerenergy.com/.

[30] https://www.makwater.com.au/.

[31] A. M. Eltamaly, E. Ali, M. Bumazza, S. Mulyono, and M. Yasin, "Optimal design of hybrid renewable energy system for a reverse osmosis desalination system in Arar, Saudi Arabia," *Arabian Journal for Science and Engineering*, vol. 46, no. 10, pp. 9879–9897, 2021.

[32] W. Gocht, A. Sommerfeld, R. Rautenbach et al., "Decentralized desalination of brackish water by a directly coupled reverse-osmosis-photovoltaic-system-a pilot plant study in Jordan," *Renewable Energy*, vol. 14, no. 1-4, pp. 287–292, 1998.

[33] A. A. E. B. A. El Halim, Y. F. Nassar, H. J. El-Khozondar, and E. H. E. Bayoumi, "Fast charging of lithium-ion battery for electric vehicles application," in *2023 8th International Engineering Conference on Renewable Energy & Sustainability (ieCRES)*, pp. 1–6, Gaza, Palestine, State of, May 2023.

[34] H. Rezk, M. Al-Dhaifallah, Y. B. Hassan, and H. A. Ziedan, "Optimization and energy management of hybrid photovoltaic-diesel-battery system to pump and desalinate water at isolated regions," *IEEE Access*, vol. 8, pp. 102512–102529, 2020.

[35] S. Upadhyay and M. P. Sharma, "Selection of a suitable energy management strategy for a hybrid energy system in a remote rural area of India," *Energy*, vol. 94, pp. 352–366, 2016.

[36] M. P. Bonkile and V. Ramadesigan, "Effects of sizing on battery life and generation cost in PV–wind battery hybrid systems," *Journal of Cleaner Production*, vol. 340, article 130341, 2022.

[37] R. Babaei, D. S.-K. Ting, and R. Carriveau, "Feasibility and optimal sizing analysis of stand-alone hybrid energy systems coupled with various battery technologies: a case study of Pelee Island," *Energy Reports*, vol. 8, pp. 4747–4762, 2022.

[38] N. Ganjei, F. Zishan, R. Alayi et al., "Designing and sensitivity analysis of an off-grid hybrid wind-solar power plant with diesel generator and battery backup for the rural area in Iran," *Journal of Engineering*, vol. 2022, Article ID 4966761, 14 pages, 2022.

[39] R. M. Ghoniem, A. Alahmer, H. Rezk, and S. As'ad, "Optimal design and sizing of hybrid photovoltaic/fuel cell electrical power system," *Sustainability*, vol. 15, no. 15, article 12026, 2023.